DNA strand breaks induced by near-zero-electronvolt electron attachment to pyrimidine nucleotides

Xiaoguang Bao[†], Jing Wang[‡], Jiande Gu[†‡§], and Jerzy Leszczynski[‡§]

[†]Drug Design and Discovery Center, State Key Laboratory of Drug Research, Shanghai Institute of Materia Medica, Shanghai Institutes for Biological Sciences, Chinese Academy of Sciences, Shanghai 201203, People's Republic of China; and [‡]Computational Center for Molecular Structure and Interactions, Department of Chemistry, Jackson State University, Jackson, MS 39217

Edited by Henry Schaefer III, University of Georgia, Athens, GA, and accepted by the Editorial Board February 23, 2006 (received for review December 2, 2005)

To elucidate the mechanism of DNA strand breaks by low-energy electrons (LEE), theoretical investigations of the LEE attachment-induced $C_{5'}$—$O_{5'}$ σ bond breaking of pyrimidine nucleotides (5′-dCMPH and 5′-dTMPH) were performed by using the B3LYP/DZP++ approach. The results indicate that the pyrimidine nucleotides are able to capture electrons characterized by near-0-eV energy to form electronically stable radical anions in both the gas phase and aqueous solution. The mechanism of the LEE-induced single-strand bond breaking in DNA might involve the attachment of an electron to the bases of DNA and the formation of base-centered radical anions in the first step. Subsequently, these radical anions undergo either C—O or glycosidic bond breaking, yielding neutral ribose radical fragments and the corresponding phosphoric anions or base anions. The C—O bond cleavage is expected to dominate because of its low activation energy. In aqueous solutions, the significant increases in the electron affinities of pyrimidine nucleotides ensure the formation of electronically more stable radical anions of the nucleotides. The low activation energy barriers for the $C_{5'}$—$O_{5'}$ bond breaking predicted in this work are relevant when the counterions are close enough to the phosphate moiety of DNA.

low-energy electrons attachment

DNA strand breaks induced by low-energy electrons (LEE) are of crucial importance because such electrons are produced in significant amounts during ionizing radiation (1). Recently, both the experimental investigations of different DNA fragment samples and theoretical studies on different models have demonstrated that, at very low energies, electrons may induce strand breaks in DNA by means of dissociative electron attachment (2–14). A detailed understanding of this LEE-induced DNA damage is essential for the advancement of global models of cellular radiolysis and for the development of more efficient methods of radiotherapy.

Based on experimental observations and theoretical rationales, different DNA strand-breaking mechanisms have been proposed (7, 9, 11, 14). These mechanisms are extremely valuable for understanding the nature of DNA strand breaks by LEE.

Experimental and theoretical investigations of the base-releasing process of pyrimidine nucleosides (9, 14) have suggested that at the nascent stage the excess electron resides on the π^* orbital of pyrimidine in the radical anion, forming an electronically stable radical anion. Subsequently, the glycosidic bond breaks to release the free pyrimidine anions and the 2-deoxyribose radical.

Theoretical studies of the sugar–phosphate–sugar moiety were performed by Li, Sevilla, and Sanche (7) and by Simons and coworkers (11). Based on the density functional theory (DFT) calculations of the gas-phase model, Li, Sevilla, and Sanche (7) proposed that the near-0-eV (1 eV = 1.602×10^{-19} J) electron may be captured first by the phosphate, forming a phosphate-centered radical anion. The subsequent $C_{3'}$—$O_{3'}$ or $C_{5'}$—$O_{5'}$ σ bond breaking was estimated to have an energy barrier of $\approx$10 kcal/mol. However, the theoretical study of Simons and coworkers (11) suggested that electrons with kinetic energies near 0 eV cannot attach directly at a significant rate to the phosphate units. It should be noted that the nucleic acid bases were excluded from the model considered in their study. The small values of electron affinity [−0.003; 0.033 eV (7)] of the sugar–phosphate–sugar model seem to suggest that the LEE might be trapped in the pyrimidine bases [with electron affinities of 0.2∼0.3 eV (15, 16)] instead of in the phosphate group in DNA species.

By using the 2′-deoxycytidine-3′-monophosphate (3′-dCMPH) molecule (10, 11, 13) and the 2′-deoxythymidine-3′-monophosphate molecule (12) as models, Simons' group carefully examined the $C_{3'}$—$O_{3'}$ bond-breaking processes in pyrimidine nucleotides. They concluded that the very-low-energy electrons can attach to the π^* orbitals of the DNA bases and undergo $C_{3'}$—$O_{3'}$ bond cleavage in an aqueous solution (10, 12, 13). Their results also suggest that in the absence of stabilization due to interactions with the solvent, the base-hosted radical anions are electronically unstable (characterized by negative values for electron affinity) (10–12). However, both experimental studies of DNA (15) and RNA (5) fragments and higher-level theoretical investigations indicate unambiguously the positive electron affinities for the pyrimidine bases, the pyrimidine nucleosides, and the pyrimidine nucleotides in the gas phase (14, 16–18). Moreover, recent experiments (0- to 4-eV electron-induced DNA strand breaks) performed by Sanche's group suggest that the DNA single-strand breaks are initiated by electron attachment to the bases in the gas phase (19).

With the reliably calibrated B3LYP/DZP++ approach, the electron affinity of 3′-dCMPH and its phosphate deprotonated anion (3′-dCMP$^-$) have been studied by Schaefer and coworkers (18). This investigation reveals that 3′-dCMPH is able to capture near-0-eV electron to form a stable radical anion in both the gas phase and in an aqueous solution. This pyrimidine-based radical anion is electronically stable enough to undergo the subsequent phosphate–sugar C—O σ bond-breaking process or the glycosidic bond cleavage process.

To elucidate the mechanism of DNA strand breaks by LEE, a reliable description of the properties of the radical anions of the nucleotides and the accurate determination of the activation energy barrier of the corresponding bound rupture is necessary. Here, we report theoretical investigations of LEE attachment-induced $C_{5'}$—$O_{5'}$ σ bond breaking of pyrimidine nucleotides.

Conflict of interest statement: No conflicts declared.

This paper was submitted directly (Track II) to the PNAS office. H.S. is a guest editor invited by the Editorial Board.

Abbreviations: au, atomic units; LEE, low-energy electrons; NPA, natural population analysis; SOMO, singly occupied molecular orbital; VDE, vertical detachment energies; VEA, vertical electron affinity; ZPE, zero point energy correction; 3′-dCMPH, 2′-deoxycytidine-3′-monophosphate; 5′-dCMP, 2′-deoxycytidine-5′-monophosphate; 5′-dCMPH, protonated form of 5′-dCMP; 5′-dTMPH, protonated form of 2′-deoxythymidine-5′-monophosphate.

[§]To whom correspondence may be addressed. E-mail: jiandegush@go.com or jerzy@ccmsi.us.

www.pnas.org/cgi/doi/10.1073/pnas.0510406103

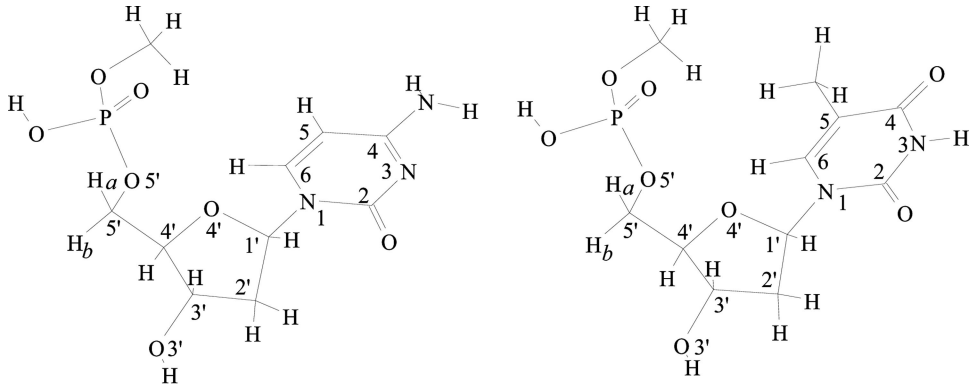

5′-dCMPH 5′-dTMPH

Scheme 1. Molecular structure and labels of the model compounds 5′-dCMPH and 5′-dTMPH.

The 2′-deoxycytidine-5′-monophosphate (5′-dCMP) system and the 2′-deoxythymidine-5′-monophosphate (5′-dTMP) system in their protonated forms (denoted as 5′-dCMPH and 5′-dTMPH) have been selected as models because the phosphoryl groups are usually attached to the oxygen atom of the 5′-hydroxyl group in naturally occurring nucleotides. (For a better description of the influence of the 3′-5′ phosphodiester linkage in DNA, the $-OPO_3H$ moiety was terminated with CH_3 group; see Scheme 1.) This model complements the previous studies of the 3′-monophosphate ester of the 2′-deoxyribonucleosides of cytosine and thymine (10–13, 18) and provides information directly related to the important building blocks of DNA.

A reliable description of the properties of the radical anions of the nucleotides and the accurate determination of the activation energy barrier of the corresponding bond rupture depend on the theoretical methods chosen. The recent development of a comprehensive density functional theory bracketing technique (20) allows the adiabatic electron affinity (EA_{ad}) values for the DNA and RNA bases close to zero ($\pm$0.3 eV) with the ordering U > T > C $\sim$ G > A, which corresponds well with the experimental data (15) to be predicted. With the reliably calibrated B3LYP/DZP++ approach, accurate predictions of the electron affinities of the 2′-deoxyribonucleosides and the 2′-deoxythymidine-2′-deoxyadenosine pairs have been accomplished (17, 21). In accord with these previous successful applications, the B3LYP/DZP++ method also was used in this study.

Results and Discussion

The mechanism of the LEE-induced single-strand bond breaking in DNA is proposed as follows (Scheme 2). The electrons attach to the DNA bases, forming the base-centered radical anions of the nucleotides in the first step. Then, these electronically stable radical anions undergo the C—O bond breaking and yield neutral ribose radical fragments and the corresponding phosphoric anions.

Energy Profiles. ***Electron affinities of 5′-dCMPH and 5′-dTMPH.*** The electron attachment and detachment energies of the pyrimidine nucleotides are summarized in Table 1. The EA_{ad} of 5′-dCMPH and 5′-dTMPH have been predicted to be 0.34 and 0.44 eV, respectively. These values are almost the same as those of the corresponding 2′-deoxyribonucleosides (0.33 eV for dC and 0.44 eV for dT) (17). However, the EA_{ad} of 5′-dCMPH is 0.10 eV lower than that of 3′-dCMPH (18). Notice that the proton at the O5′ position is H-bonded to the base on which the excess electron is located in the 3′-dCMPH$^-$ radical anion. (This intramolecular H-bond also exists in dC and dT.) The EA_{ad} decrease of 5′-dCMPH is mainly due to the absence of this intramolecular H-bonding in the 5′-dCMPH radical anion. The effect of the phosphate esterified at the O3′ position is to increase the EA_{ad} of the corresponding parent compounds by $\approx$0.10 $\sim$ 0.11 eV. Accordingly, the EA_{ad} of 3′-dTMPH should be $\approx$0.55 eV. Because the phosphate esterification at the O5′ position eliminates the intramolecular H-bond described above, the EA_{ad} of the cytidine 3′,5′-diphosphoric acid and thymidine 3′,5′-diphosphoric acid is expected to have the same value as that of 3′-dCMPH and 3′-dTMPH, respectively. Therefore, the electron affinity of the nucleotides might follow the order: thymidine 3′,5′-diphosphoric acid $\sim$ 3′-dTMPH > cytidine 3′,5′-diphosphoric acid $\sim$ 3′-dCMPH $\sim$ 5′-dTMPH > 5′-dCMPH.

The vertical electron affinity (VEA) determines the energy needed for a fast electron capture step in the formation of anions (8, 18). The small negative VEA value of $-$0.11 eV for 5′-dCMPH and the almost-zero VEA value (0.01 eV) for 5′-dTMPH suggest that both neutralized 5′-dCMPH and 5′-dTMPH species can capture near-0-eV electron in the gas phase. It should be noted that the VEA of 3′-dCMPH (0.15

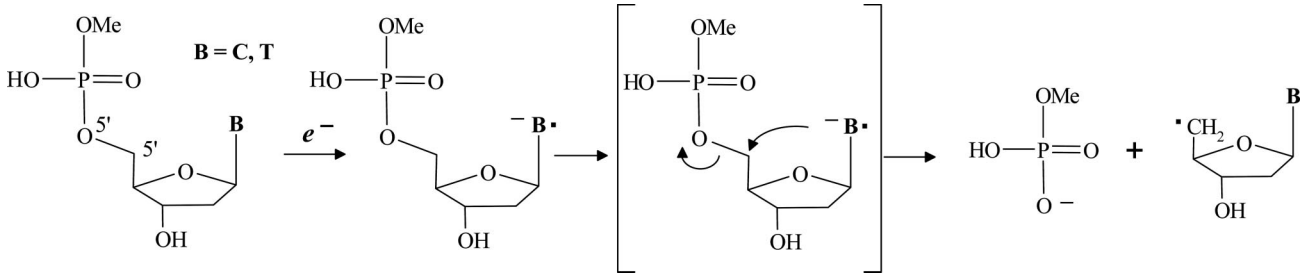

Scheme 2. Proposed mechanism of the LEE-induced single-strand bond breaking in pyrimidine nucleotides.

Table 1. Electron attachment energies for 5′-dCMPH and the 5′-dTMPH

Process	EA_{ad}	VEA†	VDE‡
Gas phase			
5′-dCMPH → 5′-dCMPH$^-$	0.20 (0.34)	−0.11	0.85
5′-dTMPH → 5′-dTMPH$^-$	0.28 (0.44)	0.01	0.99
3′-dCMPH → 3′-dCMPH$^-$	0.33 (0.44)§	0.15§	1.28§
Aqueous solution¶			
5′-dCMPH → 5′-dCMPH$^-$	1.89	1.40	2.45
5′-dTMPH → 5′-dTMPH$^-$	1.96	1.53	2.60
3′-dCMPH → 3′-dCMPH$^-$	2.18§	1.72§	2.97§

Values are in eV. The values with zero point correction are given in parentheses.

†VEA = *E*(neutral) − *E*(anion); the energies are evaluated based on the optimized neutral structures.

‡VDE = *E*(neutral) − *E*(anion); the energies are evaluated based on the optimized anion structures.

§Ref. 18.

¶Polarizable continuum model (*PCM*), using water as solvent with $\varepsilon = 78.39$.

eV) (18), which is ≈0.26 eV higher than that of 5′-dCMPH and ≈0.14 eV higher than that of 5′-dTMPH, suggests that 3′-dCMPH is even more likely to capture a free electron.

To estimate the electron autodetachment ability of the radical anion of the nucleotides, the vertical detachment energies (VDE) of the 5′-dCMPH$^-$ and 5′-dTMPH$^-$ radical anions were calculated based on the optimized radical anion structure of the corresponding species. The VDE is evaluated to be 0.85 eV for 5′-dCMPH$^-$ and 0.99 eV for 5′-dTMPH$^-$. For comparison, the VDE of the dC$^-$ nucleoside radical anion is 0.72 eV, and that of dT$^-$ is 0.94 eV (17). Conversely, the VDE is significantly higher for 3′-dCMPH$^-$ (1.28 eV) (18). In this regard, the radical anions of the pyrimidine-5′-monophosphate are electronically more stable than the corresponding nucleosides but less stable than the 3′-monophosphate nucleotides. With the VDE value of 0.85 eV (≈19.6 kcal/mol), electron autodetachment might happen during the subsequent glycosidic bond cleavage process (with an activation energy of 0.94 eV or 21.6 kcal/mol for dC$^-$) (14) in 5′-dCMPH$^-$. Conversely, one may expect that the 5′-dTMPH radical anion (the VDE value of 0.99 eV or 22.8 kcal/mol) should be electronically stable enough to undergo the subsequent glycosidic bond cleavage process (with an activation energy of 0.82 eV or 18.9 kcal/mol) (14).

An interaction with a solvent remarkably improves the ability of 5′-dCMPH and 5′-dTMPH to capture an electron. For the formation of the 5′-dCMPH radical anion, the EA_{ad} and VEA values are 1.89 and 1.40 eV increased by 1.69 and 1.51 eV, respectively, because of the solvent effects. The solvent effects also significantly increase the electronic stability of the 5′-dCMPH radical. The VDE of 5′-dCMPH$^-$ in an aqueous solution is predicted to be 2.45 eV (1.69 eV larger than in the gas phase). It is interesting to notice that the increase of the EA_{ad}, the VEA, and the VDE of 5′-dCMPH caused by the solvent effects is very close to the corresponding increase in the 3′-dCMPH compound (18) (1.7 eV for EA_{ad}, 1.5 eV for VEA, and 1.7 eV for VDE). A similar tendency also is revealed for 5′-dTMPH. The EA_{ad}, VEA, and VDE values are 1.96, 1.53, and 2.60 eV, respectively, for 5′-dTMPH in aqueous solutions.

Activation energies of the $C_{5'}$—$O_{5'}$ σ bond-breaking process in the radical anions of 5′-dCMPH and 5′-dTMPH. To explore the potential surface for the $C_{5'}$—$O_{5'}$ σ bond cleavage process, the transition states for the radical anions of both 5′-dCMPH and 5′-dTMPH have been located. These transition states are characterized by the existence of a single imaginary vibrational frequency, which amounts to 858*i* cm^{-1} for 5′-dCMPH$^-$ and to 758*i* cm^{-1} for 5′-dTMPH$^-$. The normal mode corresponding to the imaginary vibrational

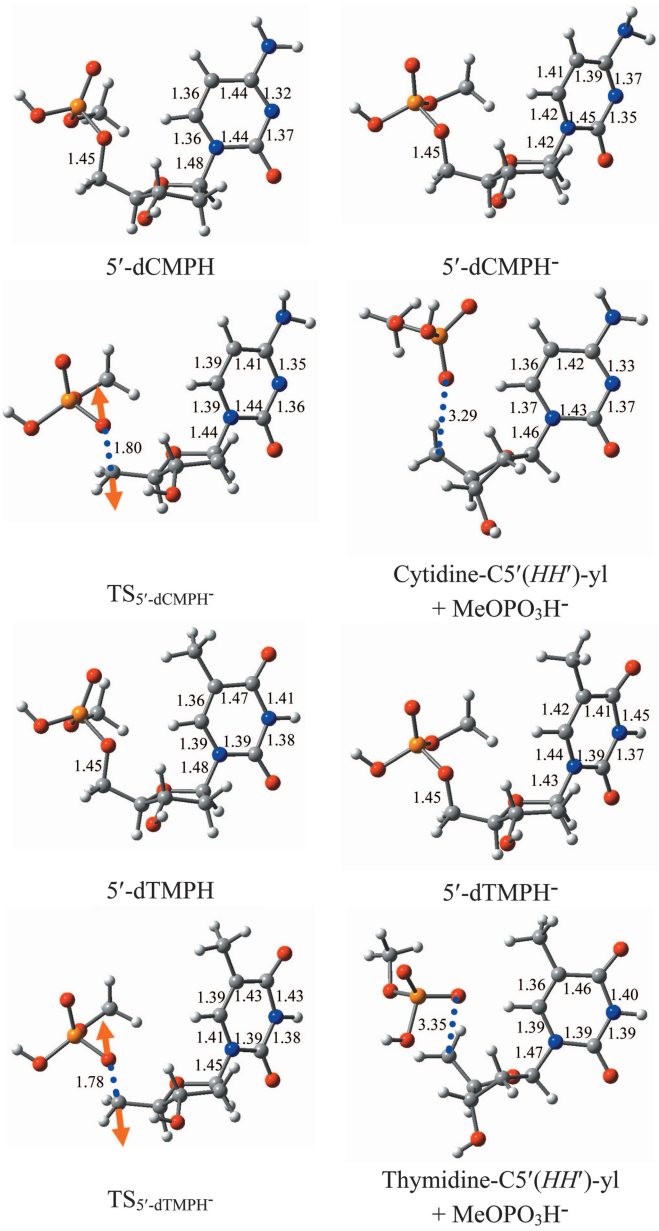

Fig. 1. The optimized structures of the neutral molecules, the radical anions, the $C_{5'}$—$O_{5'}$ bond-breaking transition states, and the corresponding bond-broken products of 5′-dCMPH and 5′-dTMPH. Bond distances are in Å. Orange arrows in the transition states represent the single imaginary frequency-related vibration mode. Red represents oxygen, gray is carbon, blue is nitrogen, orange is phosphorous, and white is hydrogen.

frequency characterizes the $C_{5'}$—$O_{5'}$ σ bond breaking (Fig. 1). The activation energy of the $C_{5'}$—$O_{5'}$ σ bond cleavage process has been predicted to be 14.3 kcal/mol or 0.64 eV (Table 2) [without the zero point energy correction (ZPE)] for the radical anion 5′-dCMPH$^-$. As a comparison, the activation energy needed for the N1-glycosidic bond breaking in dC$^-$ is 21.6 kcal/mol (0.94 eV), ≈7.3 kcal/mol higher (14). Therefore, the N1-glycosidic bond breaking is unlikely to happen in 5′-dCMPH$^-$ unless the phosphate group esterized on O5′ could significantly lower the activation energy of the glycosidic bond-breaking process. The energy barrier of the $C_{5'}$—$O_{5'}$ σ bond rupture has been found to be 13.8 kcal/mol or 0.60 eV (without ZPE correction) for the radical anion 5′-dTMPH$^-$, slightly lower

Table 2. Energy properties of the radical anions, the transition states, and the $C_{5'}$—$O_{5'}$ σ bond-broken complexes of the pyrimidine nucleotides

Species	*E*, hartree	ΔE, kcal/mol	ΔE^0, kcal/mol	ΔG^0, kcal/mol
5′-dCMPH$^-$	−1423.22913	0.00	0.00	0.00
$TS_{5'\text{-dCMPH}^-}$	−1423.20638	14.27 (17.97)†	12.52	12.75
		0.62 (0.78)†	**0.54**	**0.55**
Cytidine-C5′ (*HH*′)-yl	−1423.26574	−22.97 (−19.19)†	−24.40	−25.97
+ $MeOPO_3H^-$		**−1.00 (−0.83)†**	**−1.06**	**−1.13**
5′-dTMPH$^-$	−1482.45023	0.00	0.00	0.00
$TS_{5'\text{-dTMPH}^-}$	−1482.42817	13.84 (17.86)†	11.91	11.82
		0.60 (0.77)†	**0.52**	**0.51**
Thymidine-C5′ (*HH*′)-yl	−1482.48372	−21.01 (−16.05)†	−22.77	−23.19
+ $MeOPO_3H^-$		**−0.91 (−0.70)†**	**−0.99**	**−1.00**

ΔE^0, zero point energy corrected. ΔG^0, free energy difference at 298 K. The unit of the numbers in bold is eV.
†Polarizable continuum model (PCM), based on the gas-phase optimized structure and using water as solvent with $\varepsilon = 78.39$.

than that of 5′-dCMPH$^-$. Notice that the energy barrier for the N1-glycosidic bond breaking in dT$^-$ is 18.9 kcal/mol (0.82 eV) (14), and the N1-glycosidic bond-breaking process also is not able to compete with the $C_{5'}$—$O_{5'}$ σ bond rupture in 5′-dCMPH$^-$.

It is interesting to note that the $C_{3'}$—$O_{3'}$ σ bond-breaking energy barrier in the gas phase is predicted to be 15.6 kcal/mol (0.68 eV, with an incident electron energy of 0.2 eV) for the 3′-dCMPH$^-$ model (11, 13) and 13.0 kcal/mol (0.56 eV, with an incident electron energy of 0.25 eV) for the 3′-dTMPH$^-$ model (12). Our results seem to suggest that both bond-breaking processes are competitive in single-strand DNA damage, which is consistent with the previous conclusions based on the density functional theory study of the sugar–phosphate–sugar model that both the $C_{3'}$—$O_{3'}$ and $C_{5'}$—$O_{5'}$ σ bonds have a similar energy barrier ≈10 kcal/mol (0.43 eV) for the bond rupture (7).

The solvent effects raise the $C_{5'}$—$O_{5'}$ σ bond-breaking energy barrier by up to 18.0 kcal/mol (0.78 eV) for 5′-dCMPH$^-$ and to 17.9 kcal/mol (0.78 eV) for 5′-dTMPH$^-$. Note that the activation energies for protonation of the radical anion of thymine are <15.6 kcal/mol or even lower (22), and the $C_{5'}$—$O_{5'}$ σ bond breaking is therefore unlikely to occur in aqueous solutions.

Geometries and Charge Distributions. The optimized structures of the neutral molecules, the radical anions, the $C_{5'}$—$O_{5'}$ σ bond cleavage related transition states, and the $C_{5'}$—$O_{5'}$ bond-broken products of 5′-dCMPH and 5′-dTMPH are depicted in Fig. 1, along with the important geometric parameters. The excess electron attachment to the neutral species has little influence on the $C_{5'}$—$O_{5'}$ bond length in the radical anions. However, it slightly shortens the N1-glycosidic bond in 5′-dCMPH$^-$ (0.06 Å shorter compared with the neutral species) and 5′-dTMPH$^-$ (0.04 Å shorter). Consistent with the previous studies of the nucleosides (17) and 3′-dCMPH (18), the significant bond length alterations due to the electron attachment can be found in the structure of the bases, suggesting that the excess electron is mainly located on the bases. In the transition state, the $C_{5'}$—$O_{5'}$ bond length elongates to 1.80 Å in the 5′-dCMPH$^-$ radical anion and 1.78 Å in 5′-dTMPH$^-$. This bond distance is ≈0.10 Å longer than the values predicted based on the sugar–phosphate–sugar model for the $C_{5'}$—$O_{5'}$ bond rupture (7), whereas it is ≈0.10 Å shorter than that of $C_{3'}$—$O_{3'}$ in 3′-dCMPH (10–13). The dihedral angle around C5′ ($D_{Ha\text{-}Hb\text{-}C4'\text{-}C5'}$) amounts to 24.2° in the transition state of 5′-dCMPH$^-$ and 23.7° in 5′-dTMPH$^-$. This dihedral angle is 33.4° in the stable form of 5′-dCMPH$^-$ (33.5° in that of 5′-dCMPH$^-$) and is ≈2.1° in the $C_{5'}$—$O_{5'}$ bond-broken products [neutral 2′-deoxycytidine-C5′(*HH*′)-yl and 2′-deoxythymidine-C5′(*HH*′)-yl radicals]. An approximate reduction of 10° in the $D_{Ha\text{-}Hb\text{-}C4'\text{-}C5'}$ value indicates the sp^3 to sp^2 transformation in the electron state of C5′ in the bond-breaking procedure. Consequently, one can expect that the unpaired electron locates on the carbon atom at the 5′ position in the bond-ruptured products.

Consistent with the geometric changes, the results of a natural population analysis (NPA) for the charge distribution reveal that the excess electron is mainly located on the bases in the radical anions of the nucleotides (Table 3). The NPA charge on the cytosine base moiety amounts to −1.12 atomic units (au) in the 5′-dCMPH$^-$ radical anion, which is approximately −0.82 au more negatively charged compared with that in the neutral molecule 5′-dCMPH (−0.30 au). In the $C_{5'}$—$O_{5'}$ bond-broken product, the extra negative charge locates on the phosphate group; the NPA charge amounts to −0.96 au. The charge distribution on the cytosine moiety is −0.30 au, and that on the sugar fragment is 0.26 au in the neutral 2′-deoxycytidine-C5′(*HH*′)-yl radical. These results are similar to those from the

Table 3. NPA charge distributions of the neutral molecules, the radical anions, the transition states, and the $C_{5'}$—$O_{5'}$ σ bond-broken complexes of the pyrimidine nucleotides

Species	Base	Ribose	Phosphate
5′-dCMPH	−0.30	0.67	−0.37
5′-dCMPH$^-$	−1.12	0.50	−0.38
$TS_{5'\text{-dCMPH}^-}$	−0.76	0.39	−0.63
Cytidine-C5′ (*HH*′)-yl + $MeOPO_3H^-$	−0.30 (−0.28)†	0.26 (0.28)†	−0.96
5′-dTMPH	−0.30	0.67	−0.37
5′-dTMPH$^-$	−1.15	0.53	−0.38
$TS_{5'\text{-dTMPH}^-}$	−0.77	0.39	−0.62
Thymidine-C5′ (*HH*′)-yl + $MeOPO_3H^-$	−0.31 (−0.29)†	0.27 (0.29)†	−0.96

†NPA charge distributions of the corresponding nucleosides neutral species (see ref. 17).

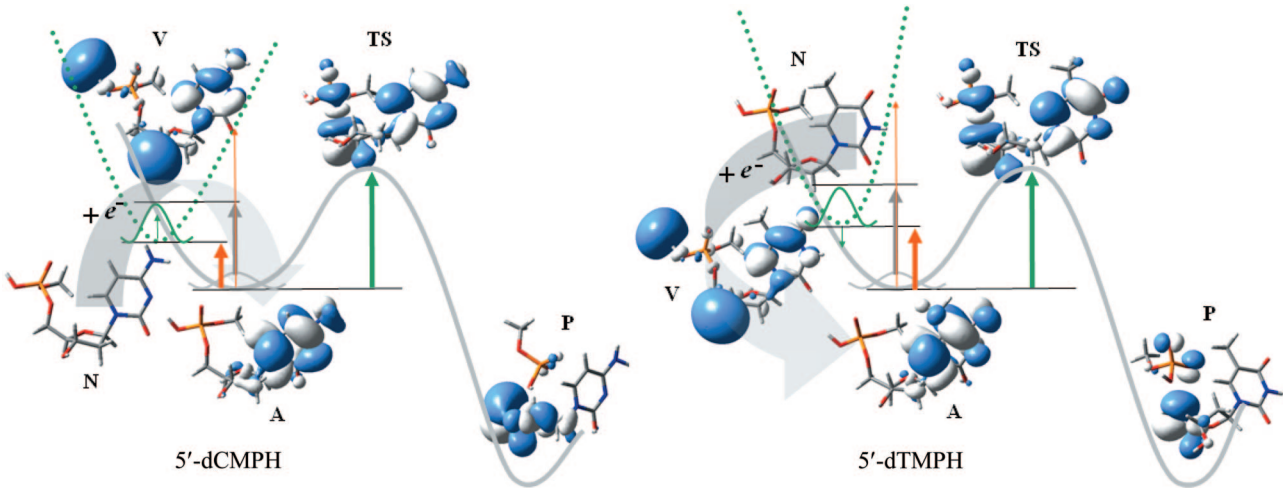

Fig. 2. The distribution of the unpaired electron along the LEE-induced $C_{5'}$—$O_{5'}$ bond-breaking pathway of the nucleotides. A green dotted line represents the potential energy surface of neutral 5′-dCMPH or 5′-dTMPH; a gray solid line represents the potential energy surface of radical anion 5′-dCMPH$^-$ or 5′-dTMPH$^-$. A thin green arrow stands for VAE; a thin orange arrow is for VDE; a thick orange arrow is for ZPE-uncorrected EA_{ad}; a thick gray arrow is for ZPE-corrected EA_{ad}; and a thick green arrow is for the activation energy. N, neutral species; A, stable radical anion; V, electron vertical attached radical anion; TS, transition state; and P, bond-broken product.

study of the nucleosides (17). A charge transfer from the base moiety to the phosphate group happens during the $C_{5'}$—$O_{5'}$ bond-breaking process as indicated by the NPA analysis. In the transition state structure for the $C_{5'}$—$O_{5'}$ bond breaking of 5′-dCMPH$^-$, the NPA charge on cytosine increases to −0.76 au (a 0.36 au increase), whereas the charge on the phosphate fragment decreases to −0.63 au (a −0.25 au decrease). In this transition state, a noticeable positive charge decrease on ribose (0.11 au less compared with that in the radical anion 5′-dCMPH$^-$) seems to suggest that the sugar facilitates the charge transfer during the $C_{5'}$—$O_{5'}$ bond-breaking process. As expected, the features of the charge distribution in 5′-dTMPH species are very close to those in 5′-dCMPH. A little more negative charge distribution on the thymine moiety in 5′-dTMPH$^-$ (−1.15 au on thymine vs. −1.12 au on cytosine) corresponds to the relatively larger electron affinity of thymine.

An analysis of the singly occupied molecular orbitals (SOMOs) provides insights into the electron attachment and the bond-breaking mechanisms. Fig. 2 illustrates the distribution of the unpaired electron along the LEE-induced $C_{5'}$—$O_{5'}$ bond-breaking pathway of the nucleotides. The SOMOs of the electron vertical attached state (the less-stable anion radical with the geometry of the stable neutral species) displays the partly dipole bound feature (15) of the radical anions (Fig. 2). After structure relaxation, the excess electron locates on the π^* orbital of the base, forming energetically more stable covalent bound radical anions 5′-dCMPH$^-$ and 5′-dTMPH$^-$, which resemble the radical anions of nucleosides (14, 17) and of 3′-dCMPH (18) in the previous studies.

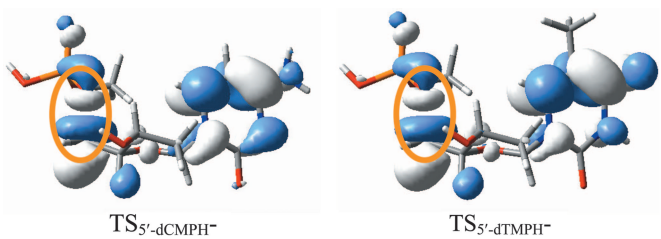

Fig. 3. The SOMOs of the transition states of the 5′-dCMPH and 5′-dTMPH radical anions. The typical characteristics of the σ antibond orbital along the $C_{5'}$—$O_{5'}$ bond are shown in the orange circle.

One of the important conclusions in the study of the N1-glycosidic bond dissociation in the pyrimidine nucleosides is that the excess negative charge is partly located on the bond to be broken (14). The SOMO of the transition states of 5′-dCMPH$^-$ and 5′-dTMPH$^-$ in Fig. 3 illustrate the similar characteristics of the charge-induced bond dissociation. The antibonding orbital of the $C_{5'}$—$O_{5'}$ bond can be recognized clearly in the SOMO of the transition states. This antibonding orbital partly occupied by one electron might be one of the important features of the negative-charge-induced bond dissociation.

The SOMO of the $C_{5'}$—$O_{5'}$ bond-broken products confirms that the radical resides on the C5′ of the 2′-deoxycytidine-C5′(*HH′*)-yl and 2′-deoxythymidine-C5′(*HH′*)-yl radicals. It is interesting to notice that in the bond-broken products of the pyrimidine nucleosides, the radical is mainly on the C1′ of the sugar, whereas the negative charge resides on the leaving bases (14). One might expect that the neutral ribose fragments should be the main radical hosts in the bond-broken products of the LEE-induced DNA damages.

Conclusions

The results of our study along with the findings of the earlier investigations (14–18) indicate that the pyrimidine nucleotides are able to capture the near-0-eV electron to form the electronically stable radical anions in both the gas phase and in aqueous solution. The electron affinities of the nucleotides follow the order: thymidine 3′,5′-diphosphoric acid ~ thymidine-3′-monophosphoric acid > cytidine 3′,5′-diphosphoric acid ~ cytidine-3′-monophosphoric acid ~ thymidine-5′-monophosphoric acid > cytidine-5′-monophosphoric acid.

One of the possible mechanisms for the LEE-induced single-strand bond breaking in DNA could involve the electron's attachment to the DNA bases and the formation of the base-centered radical anions of the nucleotides in the first step. Subsequently, these electronically stable radical anions are capable of undergoing either C—O or glycosidic bond breaking, producing the neutral ribose radical fragments and the corresponding phosphoric anions or base anions. Nevertheless, the C—O bond cleavage is expected to dominate because its activation energy is relatively lower than that of the glycosidic bond rupture.

In aqueous solutions, the significant increases in the electron affinities of the pyrimidine nucleotides ensure the formation of the electronically more stable radical anions of the nucleotides. However, because of the solvent effects, the subsequent C—O bond cleavage might be less possible because of the energy barrier increase of 4 kcal/mol for the C—O bond breaking. Reactions with lower activation barriers such as protonation of the radical anions might remove the charge before possible cleavage reactions (22).

In living systems, the phosphates of the nucleotides could be either negatively charged or neutralized by counterions such as the Na^+ and K^+ cations. Although the models used in this study represent situations in which counterions are closely bound to the phosphate group of DNA, the finding that the electron affinities of the nucleotides are independent of the counterions in aqueous solutions in the previous study (18) ensures the existence of electronically stable base-centered radical anions of nucleotides in nature. As for the C—O bond breaking, the activation energy barriers are expected to be higher in the case where counterions are far away from the phosphate group. The activation energy barriers for the $C_{5'}$—$O_{5'}$ bond breaking predicted in this study should be relevant when the counterions are close enough to the phosphate moiety of DNA.

Method of Calculation

Geometries and vibrationally zero-point corrected energies for 5′-dCMPH and 5′-dTMPH were determined by using the B3LYP (23, 24) approach. Based on the gas-phase-optimized geometries, the polarizable continuum model (PCM) (25) with a dielectric constant of water ($\varepsilon = 78.39$) was used in the calculations of the energies in a solvated environment of aqueous solution. The adiabatic electron affinity (EA_{ad}) was predicted as the difference between the total energies of the appropriate neutral and anionic species at their respective optimized geometries $EA_{ad} = E_{neut} - E_{anion}$.

The DZP++ basis sets were constructed by augmenting the Huzinaga–Dunning (26–28) set of contracted double-ζ Gaussian functions with one set of p-type polarization functions for each H atom and one set of five d-type polarization functions for each C, N, O, or P atom [$\alpha_p(H) = 0.75$, $\alpha_d(C) = 0.75$, $\alpha_d(N) = 0.80$, $\alpha_d(O) = 0.85$, $\alpha_d(P) = 0.60$]. To complete the DZP++ basis, one even-tempered diffuse s function was added to each H atom, while sets of even-tempered diffuse s and p functions were centered on each heavy atom. The even-tempered orbital exponents were determined according to the prescription of Lee and Schaefer (29). The GAUSSIAN 03 programs (30) were used in the computation.

Work in China was supported by the Chinese Academy of Sciences Knowledge Innovation Program. In the U.S., this work was supported by National Institutes of Health Grant G1 2RR13459-21 and National Science Foundation CREST Grant 9805465.

1. LaVerne, J. A. & Pimblott, S. M. (1995) *Radiat. Res.* **141,** 208–215.
2. Boudaiffa, B., Cloutier, P., Hunting, D., Huels, M. A. & Sanche, L. (2000) *Science* **287,** 1658–1660.
3. Pan, X., Cloutier, P., Hunting, D. & Sanche, L. (2003) *Phys. Rev. Lett.* **90**, 208102-1–208102-4.
4. Caron, L. G. & Sanche, L. (2003) *Phys. Rev. Lett.* **91,** 113201.
5. Hanel, G., Gstir, B., Denifl, S., Scheier, P., Probst, M., Farizon, B., Farizon, M., Illenberger, E. & Mark, T. D. (2003) *Phys. Rev. Lett.* **90,** 188104-1–188104-4.
6. Zheng, Y., Cloutier, P., Hunting, D., Wagner, J. R. & Sanche, L. (2004) *J. Am. Chem. Soc.* **126,** 1002–1003.
7. Li, X., Sevilla, M. D. & Sanche, L. (2003) *J. Am. Chem. Soc.* **125,** 13668–13669.
8. Huels, M. A., Boudaiffa, B., Cloutier, P., Hunting, D. & Sanche, L. (2003) *J. Am. Chem. Soc.* **125,** 4467–4477.
9. Abdoul-Carime, H., Gohlke, S., Fischbach, E., Scheike, J. & Illenberger, E. (2004) *Chem. Phys. Lett.* **387,** 267–270.
10. Barrios, R., Skurski, P. & Simons, J. (2002) *J. Phys. Chem. B* **106,** 7991–7994.
11. Berdys, J., Anusiewicz, I., Skurski, P. & Simons, J. (2004) *J. Am. Chem. Soc.* **126,** 6441–6447.
12. Berdys, J., Skurski, P. & Simons, J. (2004) *J. Phys. Chem. B* **108,** 5800–5805.
13. Berdys, J., Anusiewicz, I., Skurski, P. & Simons, J. (2004) *J. Phys. Chem. A* **108,** 2999–3005.
14. Gu, J., Xie, Y. & Schaefer, H. F. (2005) *J. Am. Chem. Soc.* **127,** 1053–1057.
15. Schiedt, J., Weinkauf, R., Neumark, D. & Schlag, E. (1998) *Chem. Phys.* **239,** 511–524.
16. Wesolowski, S. S., Leininger, M. L., Pentchev, P. N. & Schaefer, H. F. (2001) *J. Am. Chem. Soc.* **123,** 4023–4028.
17. Richardson, N. A., Gu, J., Wang, S., Xie, Y. & Schaefer, H. F. (2004) *J. Am. Chem. Soc.* **126,** 4404–4411.
18. Gu, J., Xie, Y. & Schaefer, H. F. (2006) *J. Am. Chem. Soc.* **128,** 1250–1252.
19. Rienstra-Kiracofe, J. C., Tschumper, G. S., Schaefer, H. F., Nandi, S. & Ellison, G. B. (2002) *Chem. Rev.* **102,** 231–282.
20. Martin, F., Burrow, P. D., Cai, A., Cloutier, P., Hunting, D. & Sanche, L. (2004) *Phys. Rev. Lett.* **93,** 068101-1–068101-4.
21. Gu, J., Xie, Y. & Schaefer, H. F. (2005) *J. Phys. Chem. B* **109,** 13067–13075.
22. Becker, D. & Sevilla, M. D. (1993) *Adv. Radiat. Biol.* **17,** 121–180.
23. Lee, T. J. & Schaefer, H. F. (1985) *J. Chem. Phys.* **83,** 1784–1794.
24. Becke, A. D. (1993) *J. Chem. Phys.* **98,** 5648–5652.
25. Cossi, M., Barone, V., Cammi, R. & Tomasi, J. (1996) *Chem. Phys. Lett.* **255,** 327–335.
26. Huzinaga, S. (1965) *J. Chem. Phys.* **42,** 1293–1302.
27. Dunning, T. H. (1970) *J. Chem. Phys.* **53,** 2823–2833.
28. Dunning, T. H. & Hay, P. J. (1977) in *Modern Theoretical Chemistry*, ed. Schaefer, H. F. (Plenum, New York), Vol. 3, pp. 1–27.
29. Lee, C., Yang, W. & Parr, R. G. (1988) *Phys. Rev. B* **37,** 785–789.
30. Frisch, M. J., Trucks, G. W., Schlegel, H. B., Scuseria, G. E., Robb, M. A., Cheeseman, J. R., Montgomery, J. A., Vreven, T., Kudin, K. N., Burant, J. C., *et al*. (2003) GAUSSIAN 03 (Gaussian, Pittsburgh), Revision C.02.